Gaussian process repetitive control

Beyond periodic internal models through kernels

Mooren, Noud; Witvoet, Gert; Oomen, Tom

Citation (APA)
Mooren, N., Witvoet, G., & Oomen, T. (2022). Gaussian process repetitive control: Beyond periodic internal models through kernels. *Automatica*, *140*, Article 110273. https://doi.org/10.1016/j.automatica.2022.110273

Important note
To cite this publication, please use the final published version (if applicable).
Please check the document version above.

Gaussian process repetitive control: Beyond periodic internal models through kernels ☆

Noud Mooren [a,*], Gert Witvoet [a,b], Tom Oomen [a,c]

[a] *Control Systems Technology Section, Department of Mechanical Engineering, Eindhoven University of Technology, Eindhoven, The Netherlands*
[b] *Optomechatronics Department, TNO, Delft, The Netherlands*
[c] *Delft Center for Systems and Control, Delft University of Technology, Delft, The Netherlands*

ABSTRACT

Repetitive control enables the exact compensation of periodic disturbances if the internal model is appropriately selected. The aim of this paper is to develop a novel synthesis technique for repetitive control (RC) based on a new more general internal model. By employing a Gaussian process internal model, asymptotic rejection is obtained for a wide range of disturbances through an appropriate selection of a kernel. The implementation is a simple linear time-invariant (LTI) filter that is automatically synthesized through this kernel. The result is a user-friendly design approach based on a limited number of intuitive design variables, such as smoothness and periodicity. The approach naturally extends to reject multi-period and non-periodic disturbances, exiting approaches are recovered as special cases, and a case study shows that it outperforms traditional RC in both convergence speed and steady-state error.

1. Introduction

Repetitive control (RC) can effectively improve positioning performance for systems that have dominant repeating errors, examples include Merry, Kessels, Heemels, van de Molengraft, and Steinbuch (2011), Shan and Leang (2012). Asymptotic rejection of repeating disturbances in RC is enabled by the internal model principle (Francis & Wonham, 1976). In particular, a disturbance model is specified as a time-domain memory loop, such that an error that is periodic with the same period can be fully compensated (Goodwin & Sin, 2014; Hara, Yamamoto, Omata, & Nakano, 1988).

Repetitive control is only applicable to periodic signals with a known period due to the traditional delay-based buffer as an internal disturbance model. A key assumption to achieving good performance is that the delay size matches the known period of the disturbance. As a result, RC is very sensitive to small variations in the disturbance period and non-periodic disturbances are even amplified (Steinbuch, 2002). This limits achievable performance in practice, e.g., if the disturbance period is uncertain, or does not fit into the delay size which is an integer multiple of the sample time. In addition, many practical applications have multiple periodic components in the error. If multiple periodic disturbances occur, then their sum may have a very large common multiple, or can even be non-periodic if there is no common multiple, i.e., a situation where traditional RC memory loops are not directly applicable.

Several modifications have been made to the memory loop in RC to improve robustness and performance. In Steinbuch (2002) and Steinbuch, Weiland, and Singh (2007) robustness for small variations in the period time is addressed by incorporating multiple memory loops referred to as higher-order RC (HORC). This results in a trade-off between period uncertainty and sensitivity to non-periodic disturbances, which can be tuned optimally as shown in Pipeleers, Demeulenaere, de Schutter, and Swevers (2008). In Cao and Ledwich (2002) an approach is presented for disturbance periods that are not an integer multiple of the sample time through interpolation. In Chang, Suh, and Oh (1998) and Zhou et al. (2007) extensions of RC are presented to learn multi-period disturbances by connecting multiple RCs, that each address a single period, in different configurations. However, the design of multi-period RC requires a sequential design procedure to take the interaction between different RCs into account,

at the expense of increased complexity in the design procedure, as shown in Blanken, Bevers, Koekebakker, and Oomen (2020). Moreover, the above approaches are extensions or combinations of the traditional delay-based non-parametric memory loop tailored towards specific refinements instead of generic approaches.

Parametric internal models for RC enable rejection of a wider class of disturbances, e.g., matched basis functions and adaptive RC approaches in Cuiyan, Dongchun, and Xianyi (2004), Pérez-Arancibia, Tsao, and Gibson (2010) and Shi, Longman, and Nagashima (2014). In this approach, a set of basis functions is defined by selecting all relevant frequencies in the error, subsequently, the corresponding coefficients are learned. This allows to learn multi-period disturbances and non-periodic disturbances, but it requires each specific frequency and its harmonics to be selected a priori.

In view of generic internal models for RC, recent developments in kernel-based approaches such as Gaussian Process (GP) regression have shown to be promising, general results include, identification and control of LTI systems (Pillonetto & De Nicolao, 2010; Scampicchio, Chiuso, Formentin, & Pillonetto, 2019), non-linear systems (Berkenkamp, Moriconi, Schoellig, & Krause, 2016; Mazzoleni, Scandella, Formentin, & Previdi, 2020). GP regression is a non-parametric approach that allows learning a wide range of functions, more specifically, a distribution over functions is learned, by specifying prior knowledge in the sense of a kernel function through hyperparameters (Murphy, 2012; Williams & Rasmussen, 2006). Gaussian processes are utilized in RC for the compensation of spatially periodic disturbances in Mooren, Witvoet, and Oomen (2020). Here, GP regression is employed with a periodic kernel to learn a continuous function from the non-equidistant observations, which is periodic in the spatial domain and potentially non-periodic in the time domain. In contrast to parametric internal models for RC, where the basis functions have to be selected explicitly, the GP is a non-parametric approach that only requires selecting a periodic kernel function with a few intuitive tuning parameters. However, the further use of GPs in time-domain RC is not yet explored and the computational complexity of GPs hampers the practical implementation.

Although recently substantial improvements have been made to the robustness and applicability of RC, a unified internal model for RC that covers a wide range of disturbances is not yet available. The aim of this paper is to present a generic internal model for RC that efficiently uses Gaussian Processes to enable the rejection of a wide variety of disturbances, including, single-period, multi-period, and non-periodic disturbances, by specifying disturbance properties in a kernel function. By learning a continuous function, the disturbance period is not restricted to be an integer multiple of the sample time allowing for rational disturbance periods, which is different in, e.g., Hara et al. (1988) and Nagahara and Yamamoto (2016). The following contributions are identified:

C1 a generic RC design framework and computationally inexpensive internal disturbance model using GP is presented, including prior selection, LTI representation, stability analysis, and a design procedure (Sections 3 and 4);

C2 performance and robustness analysis is performed, providing new insights for RC synthesis from a kernel-based perspective (Section 5); and

C3 implementation aspects that improve learning within the first period are presented (Section 6).

Several existing approaches are recovered as special cases of the presented framework, and a generic case study is performed to validate the approach.
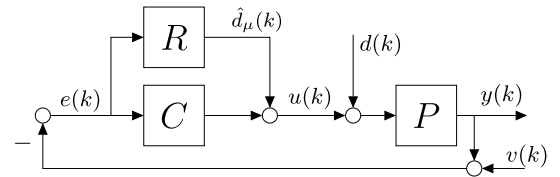

Fig. 1. Control setting with multi-period disturbance $d(k)$ with $k \in \mathbb{N}$ and repetitive controller R.

The paper is outlined as follows. In Section 2, the disturbance attenuation problem and considered class of disturbances are introduced. In Section 3, the Gaussian-process-based RC (GPRC) is developed, including LTI case and stability conditions (C1). In Section 4, design of GPRC and provides design procedure (C1). In Section 5, the performance and robustness of GPRC are analyzed, and existing methods are recovered as special cases (C2). In Section 6, learning in the first period is improved (C3). In Section 7, a case study validates the developed approach and Section 8 presents conclusions and ongoing research.

2. Problem formulation

2.1. Control setting

The considered problem is depicted in Fig. 1, where P is a discrete-time linear time-invariant (LTI) system, C is a stabilizing feedback controller, and R is an add-on type repetitive controller (RC) that is specified in the forthcoming sections. The goal is to reject the input disturbance $d(k)$ with $k \in \mathbb{Z}_{\geq 0}$, where $d(k)$ is a sampled version of a continuous disturbance $d^c(t)$ with $t \in \mathbb{R}$, i.e., $d(k) = d^c(kT_s)$. Without loss of generality the sample time is scaled to $T_s = 1$. Furthermore, noise v is present that follows an independent, identically distributed (i.i.d.) Gaussian distribution with zero mean.

Definition 1. The control goal is to asymptotically reject the disturbance-induced error $e_d(k)$, given by $e(k)$ in Fig. 1 for $v(k) = 0$, i.e.,

$$\lim_{k \to \infty} e_d(k) = 0 \tag{1}$$

by designing R. In the case that R is LTI, then

$$e_d = -\underbrace{P(I + PC)^{-1}}_{S_P} \underbrace{(I + S_P R)^{-1}}_{S_R} d \tag{2}$$

where S_R is the modifying sensitivity, that is a measure for the performance improvement through R, and S_P is the process sensitivity when $R = 0$.

Asymptotic rejection for a wide range of disturbances is obtained through a generic internal disturbance model in R which is investigated next.

Remark 1. The RC configuration in R is slightly different from the traditional one, e.g., as in Steinbuch et al. (2007). If R is linear, these are equivalent due to the commutative property of linear systems. The presented one has particular advantages in view of the GP prior as the RC output is equal to the disturbance in an ideal setting.

2.2. Internal model control

The internal model principle states that asymptotic disturbance rejection is obtained by including a model of the disturbance generating system in a stable feedback loop, see, e.g., Francis and Wonham (1976). By the final value theorem (Schiff, 1999),
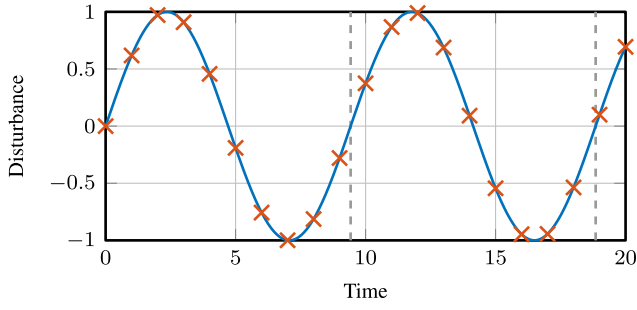
Fig. 2. Example: a continuous time disturbance $d^c(t)$ (——) with period $T = 3\pi$ from which discrete samples $d(k)$ (✕) with sample frequency 1 Hz are taken, i.e., the discrete time sequence $d(k)$ is non-periodic for all k while the continuous time signal $d^c(t)$ is periodic with the period time $T \in \mathbb{R}$.

it can be shown that a constant disturbance $d(k) = 1$ with $\mathcal{Z}$-transform $(1 - z^{-1})^{-1}$, is asymptotically rejected with a factor $(1 - z^{-1})^{-1}$ in the open-loop PC. For periodic disturbances with period $T \in \mathbb{N}$, a model of the disturbance generating system consists of a delay-based buffer z^{-N}, with $N = T$, in a feedback loop, i.e.,

$$R^{\text{conv}}(z) = \frac{z^{-N}}{1 - z^{-N}} = \frac{1}{z^N - 1}, \tag{3}$$

which is the most simple form of conventional RC, that it is often employed with a learning filter for stability, to asymptotically attenuate any disturbance with period time T, see, e.g., Goodwin and Sin (2014). However, disturbances with a rational period time $T \in \mathbb{R}$, as illustrated in Fig. 2, do not fit in these traditional buffers and require additional interpolation.

The following general class of disturbances is considered in this paper.

Definition 2. The continuous-time disturbance is defined as

$$d^c(t) = \sum_{i=1}^{n_d} d_i^c(t), \tag{4}$$

which is a multi-period disturbance consisting of $n_d \in \mathbb{N}$ periodic scalar-valued signals $d_i^c(t) \in \mathbb{R}$ that are smooth and satisfy

$$d_i^c(t) = d_i^c(t - \beta T_i), \tag{5}$$

with $\beta \in \mathbb{Z}$, and $T_i \in \mathbb{R}$ is the period time of the ith component. Moreover, the frequency content of the disturbance signal is contained below the Nyquist frequency, i.e., π, to avoid aliasing.

The disturbance (4) is a single-period disturbance if $n_d = 1$ or a multi-period disturbance with $n_d > 1$; in the latter case $d^c(t)$ is either periodic with a period equal to the least common multiple (LCM)

$$T = \text{lcm}\{T_1, T_2, \ldots, T_{n_d}\} \in \mathbb{R}, \tag{6}$$

or is non-periodic if there is no least common multiple.

Existing extensions of traditional internal models for RC that cover multi-period disturbances lead to a complicated design procedure due to interaction between different RCs, see, e.g., Blanken et al. (2020). Alternatively, the buffer size N in (3) can be chosen equal to the common multiple (6) yielding slow learning performance if T is very large. Yet, a generic internal model for the class of disturbances in Definition 2 is not available.

2.3. Gaussian process RC setup

The RC structure that is presented in this paper is shown in Fig. 3, where L is a learning filter and the proposed GP-based
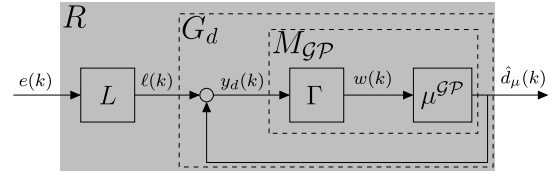

Fig. 3. Gaussian process repetitive controller R with Gaussian-process-based buffer $M_{\mathcal{GP}} = \mu^{\mathcal{GP}}\Gamma$ and internal model of the disturbance generating system G_d.

internal model of the disturbance generating system is given by G_d with $M_{\mathcal{GP}} = \mu^{\mathcal{GP}}\Gamma$ the GP-based memory. Moreover, $\Gamma \in \mathcal{RH}_\infty^{N \times 1}(z)$ is a delay line that accumulates the past $N \in \mathbb{N}$ samples of its input $y_d \in \mathbb{R}$, i.e.,

$$\Gamma := \begin{cases} x(k+1) &= Ax(k) + By_d(k) \\ w(k) &= Cx(k) + Dy_d(k), \end{cases} \tag{7}$$

where $x \in \mathbb{R}^N$ is the state, and

$$\left[\begin{array}{c|c} A & B \\ \hline C & D \end{array}\right] = \left[\begin{array}{cc|c} 0 & 0 & 1 \\ I_{N-1} & 0 & 0 \\ \hline 0 & 0 & 1 \\ I_{N-1} & 0 & 0 \end{array}\right], \tag{8}$$

which results in the vector valued signal $w(k) \in \mathbb{R}^N$. Finally, $\mu^{\mathcal{GP}} \in \mathbb{R}^{1 \times N}$ is a vector of, possibly time-varying, coefficient that are designed and formally introduced in the forthcoming sections.

2.4. Problem definition

In this paper, a systematic design approach for the repetitive controller R is presented, by developing a generic Gaussian-process-based internal disturbance model for the disturbances in Definition 2, see Fig. 3. A Gaussian process (GP) specifies disturbance properties through a kernel function and hyperparameters, which enables to model a wide range of disturbances as in Definition 2. The following requirements are addressed:

R1 asymptotic rejection for a wide range of disturbances, i.e., periodic, multi-period, and non-periodic disturbances, in the setting in Fig. 1, and

R2 a user-friendly approach for synthesizing R by specifying disturbance properties, such as periodicity and smoothness, through a kernel function.

A framework that utilizes GP-based internal models in RC to cover both R1 and R2 is presented.

3. Gaussian process buffer in repetitive control

In this section, the generalized Gaussian process repetitive control (GPRC) framework to synthesize the repetitive controller R is introduced. The GPRC setup is further outlined in Section 3.1, after which the GP internal model is presented in Section 3.2. Conditions under which GPRC is LTI and non-conservative stability conditions are provided in Sections 3.3 and 3.4 respectively, constituting contribution C1.

3.1. Gaussian process repetitive control setup

The GP-based repetitive controller R in Fig. 3 contains the GP-based disturbance model G_d that is designed using GP-regression to generate a continuous model of the true disturbance d^c. A sample of $\hat{d}^c$ is parameterized as

$$\hat{d}_\mu(k) = \mu_k^{\mathcal{GP}} w(k) \tag{9}$$

where $\mu_k^{\mathcal{GP}} \in \mathbb{R}^{1 \times N}$ are, in general, time-varying coefficients that follow from GP regression elaborated in detail in Section 3.2. Moreover, in Section 3.3 mild conditions are provided under which $\mu^{\mathcal{GP}}$ is time invariant.

The data used for GP-regression is given by the noisy data samples in

$$w(k) = \begin{bmatrix} y_d(k) & y_d(k-1) & \dots & y_d(k-N+1) \end{bmatrix}^\top \quad (10)$$

to estimate a continuous function $\hat{d}^c$ of the true disturbances d^c for compensation. To compose the data set for GP regression, define the vector with corresponding time instances

$$X(k) = \begin{bmatrix} t(k) & t(k-1) & \dots & t(k-N+1) \end{bmatrix}^\top, \quad (11)$$

constituting the data set $\mathcal{D}_N(k) = (w(k), X(k))$ that contains N pairs (y_d, t) of observations. At each sample k the data $\mathcal{D}_N(k)$ is used to perform GP regression resulting in the coefficients $\mu_k^{\mathcal{GP}}$ as shown next.

Remark 2. Note that all the past data can be used for GP regression, i.e., all samples $y_d(k')$ with $k' \in \{1, 2, \dots, k\}$ at sample k such that $w(k) \in \mathbb{R}^k$. However, here N is fixed analog to traditional RC approaches, generalization to larger buffers is conceptually straightforward, for example, using on-line GP regression (Bijl, Schön, van Wingerden, & Verhaegen, 2017; Umlauft, Beckers, Capone, Lederer, & Hirche, 2020).

3.2. Gaussian process disturbance model

The compensation signal (9) with coefficients $\mu_k^{\mathcal{GP}}$ is an estimate of the disturbance that is obtained using data and prior knowledge through GP regression. In this section, it is shown how GP regression is used to model the disturbance and consequently synthesize these coefficients.

First, consider the prior disturbance model $\hat{d}^c$ given by a GP

$$\hat{d}^c(t) \sim \mathcal{GP}(m(t), \kappa(t, t')), \quad (12)$$

that is a distribution over functions which is completely determined by its prior mean function $m(t)$ and prior covariance function $\kappa(t, t') : \mathbb{R}^n \times \mathbb{R}^m \mapsto \mathbb{R}^{n \times m}$ with n and m the size of t and t' respectively. The choice of a covariance function depends on the disturbance properties, e.g., periodicity, which is investigated in detail in Section 4.2 by taking the additive structure in (4) into account. For presentation purposes, $m(t) = 0$, the results can easily be extended for non-zero mean function, see, e.g., Murphy (2012). Next, it is shown how the prior knowledge (12) and the data $\mathcal{D}_N$ is used to compute $\mu_k^{\mathcal{GP}}$ in (9).

The data set $\mathcal{D}_N$ contains noisy observations of the model $\hat{d}^c(t)$ in (12), i.e.,

$$w(k) = \begin{bmatrix} \hat{d}^c(t(k)) \\ \hat{d}^c(t(k-1)) \\ \vdots \\ \hat{d}^c(t(k-N+1)) \end{bmatrix} + \epsilon, \quad (13)$$

where $\epsilon \sim \mathcal{N}(0_N, \sigma_n^2 I_N)$, with 0_N a matrix of zeros of size $N \times N$, that follows an independent, identically distributed (i.i.d.) Gaussian distribution with zero mean and variance σ_n^2 as a result of the noise v.

Predictions of the disturbance model for compensation can be made at arbitrary $X_* \in \mathbb{R}$, denoted by $\hat{d}^c(X_*) = \hat{d}_*^c$, based on the data $\mathcal{D}_N$ and prior (12). Moreover, for the application in RC, predictions are made at the current time, i.e., the test point becomes $X_* = t(k) \in \mathbb{Z}_{\geq 0}$ since $T_s = 1$. The joint prior distribution

$$\begin{bmatrix} w \\ \hat{d}_*^c \end{bmatrix} \sim \mathcal{N}\left(\begin{bmatrix} 0 \\ 0 \end{bmatrix}, \begin{bmatrix} K + \sigma_n^2 I_N & K_* \\ K_*^\top & K_{**} \end{bmatrix} \right), \quad (14)$$

defines the correlation between the data $w(k)$ and the test point X_*, where $K = \kappa(X, X) \in \mathbb{R}^{N \times N}$ is the covariance function κ evaluated at all pairs of (X, X), and similarly for $K_* = \kappa(X, X_*) \in \mathbb{R}^N$ and $K_{**} = \kappa(X_*, X_*) \in \mathbb{R}$. From (14) it follows that the predictive posterior distribution at the test point X_* becomes $p(\hat{d}_*^c | \mathcal{D}_N, X_*) = \mathcal{N}(\hat{d}_\mu, \Sigma)$ where

$$\hat{d}_\mu(k) = K_*^\top (K + \sigma_n^2 I_N)^{-1} w(k), \quad (15a)$$

$$\Sigma(k) = K_{**} - K_*^\top (K + \sigma_n^2 I_N)^{-1} K_*, \quad (15b)$$

are the mean and variance respectively, see, e.g., Murphy (2012, Chapter 4.3). The posterior mean $\hat{d}_\mu$ is equal to the maximum a posteriori (MAP) estimate, and is used for compensation, yielding that the coefficients $\mu_k^{\mathcal{GP}}$ in (9) are given by

$$\mu_k^{\mathcal{GP}} = K_*^\top (K + \sigma_n^2 I_N)^{-1}. \quad (16)$$

By performing GP regression (15) at each sample, updated coefficients $\mu_k^{\mathcal{GP}}$ are obtained through (16) for compensation. In contrast to traditional RC with internal disturbance model (3), GPRC enables compensation within the first period. Furthermore, by using a GP function estimator a more general setting is established in which also multi-period and non-periodic disturbances can be captured with suitable prior, as shown in Section 5.

3.3. LTI representation of GPRC

In this section, conditions are presented under which the coefficients $\mu^{\mathcal{GP}}$ in (16) are time invariant, rendering the repetitive controller in Fig. 3 to be LTI.

Assumption 1. Consider the following assumptions on the covariance function κ and training data set $\mathcal{D}_N$;

A1 the covariance function κ in (12) is a stationary function, i.e., a function of the relative difference $\tau(k) = t(k) - t'(k)$, see, e.g., Williams and Rasmussen (2006, p.82);
A2 the vector $X(k) \in \mathbb{R}^N$ in (11) contains equidistantly sampled time instances with N fixed; and
A3 the test point $X_*(k) = t(k + \alpha)$ with $\alpha \in \mathbb{Z}$ constant.

Theorem 1. *Under Assumption 1, the repetitive controller R in Fig. 3 is LTI and given by*

$$R = \frac{M_{\mathcal{GP}} L}{1 - M_{\mathcal{GP}}}, \quad (17)$$

where the GP buffer $M_{\mathcal{GP}}$ is a finite impulse response (FIR) filter

$$M_{\mathcal{GP}}(z) = \mu^{\mathcal{GP}} \Gamma(z) = \sum_{i=0}^{N-1} \mu_i^{\mathcal{GP}} z^{-i}, \quad (18)$$

with time-invariant coefficients $\mu^{\mathcal{GP}}$.

Proof. If $\mu^{\mathcal{GP}}$ in (16) is time-invariant under Assumption 1, then R in Fig. 3 is LTI and of the from (17). Hence, it is shown that (16) is time-invariant under A1–A3. First, K is obtained by evaluating the kernel function κ at all combinations of $(X(k), X(k))$ with $X(k)$ in (11), these combinations are given by

$$\tau(k) = X(k) 1_N^\top - 1_N X(k)$$
$$= \begin{bmatrix} t_k - t_k & t_k - t_{k-1} & \dots & t_k - t_{k-N+1} \\ t_{k-1} - t_k & t_{k-1} - t_{k-1} & & \vdots \\ \vdots & & \ddots & \\ t_{k-N+1} - t_k & \dots & & t_{k-N+1} - t_{k-N+1} \end{bmatrix}$$

which is Toeplitz, $1_N \in \mathbb{R}^N$ is a matrix of ones, and $t_{k-i} = t(k-i)$. Second, from assumption A2 it follows that $\tau(k) = \tau(j) \; \forall \; (k, j) \in$

$\mathbb{Z}$. Similarly for K_* that is obtained by evaluating κ at all pairs $(X(k), X_*)$ given by

$$\bar{\tau}(k) = X^\top - 1_N^\top X_* = \begin{bmatrix} X_* - t_k & \ldots & X_* - t_{k-N+1} \end{bmatrix}$$

which, under assumptions A3, satisfy that $\bar{\tau}(k) = \bar{\tau}(j) \ \forall \ (k, j) \in \mathbb{Z}$. Third, under assumption A1, the kernel matrices K and K_* are a function of $\kappa(\tau)$ and $\kappa(\bar{\tau})$ respectively. Since, τ and $\bar{\tau}$ are time-invariant, so are K and K_*, as a result, rendering (16) time invariant, such that R is of the form (17) which completes the proof.

Consequently, the RC output (9) is given by the following FIR operation

$$\hat{d}_\mu(k) = \sum_{i=0}^{N-1} \mu_i^{\mathcal{GP}} y_d(k - i), \tag{19}$$

with fixed coefficient $\mu^{\mathcal{GP}}$ that follow from (16). In addition, the internal disturbance model is now also LTI and given by

$$G_d = \frac{M_{\mathcal{GP}}}{1 - M_{\mathcal{GP}}}. \tag{20}$$

As a result, the synthesis of a generalized, possibly multi-period, RC reduces to the selection of a covariance function κ. By evaluating (16), this framework then facilitates the construction of appropriate FIR coefficients $\mu^{\mathcal{GP}}$, through which it enables efficient implementation of GPs in RC, allowing for larger flexibility, and offers superior performance in the first period due to continuous updating.

3.4. Stability analysis

In this section, the stability of GPRC with LTI repetitive controller R in (17) is analyzed in the setting in Fig. 1, resulting in non-conservative stability conditions.

Theorem 2. *Consider Fig. 1 with repetitive controller (17) in Theorem 1, a specified kernel function κ and a buffer size N. Suppose all poles of S_P and L are in the open unit disk, and the feedback loop in Fig. 1 is asymptotically stable, then the closed-loop is stable if and only if the image of $-M_{\mathcal{GP}}(z)(1 - S_P(z)L(z))$;*

- *makes no encirclements around the point -1, and*
- *does not pass through the point -1,*

as z traverses the Nyquist contour D in Fig. 4, see, Skogestad and Postlethwaite (2007).

Proof. The setting in Fig. 1 is stable if and only if $S_P \in \mathcal{RH}_\infty$ and $S_R = (1 + S_P R)^{-1} \in \mathcal{RH}_\infty$. First, S_P is proper and stable by the assumption in Theorem 2. Second, substituting R (17) in S_R (2) gives

$$S_R = \frac{1 - M_{\mathcal{GP}}}{1 - M_{\mathcal{GP}}(1 - S_P L)}, \tag{21}$$

the Nyquist theorem, see, e.g., Skogestad and Postlethwaite (2007, Theorem 4.14), states that S_R is stable if and only if the image of $-M_{\mathcal{GP}}(z)(1 - S_P(z)L(z))$ (i) encircles the point -1 in anti-clockwise direction P_{ol} times, and (ii) does not pass through the point -1 as z traverses the D, where P_{ol} is the number of poles of $-M_{\mathcal{GP}}(1 - S_P L)$ inside D.

It remains to show that $P_{ol} = 0$, i.e., there are no unstable poles in $-M(1 - S_P L)$. This holds true since $M_{\mathcal{GP}}$ is a FIR filter, see Theorem 1, with all poles in the origin, and, S_P and L are stable by the assumptions in Theorem 2, which completes the proof.
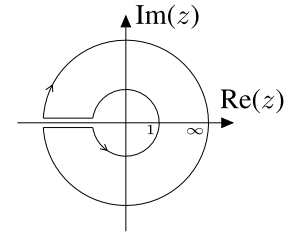

Fig. 4. Nyquist contour D with inner radius 1, outer radius infinity, and the parallel lines infinitely close to the real axis.

Theorem 2 provides a non-conservative condition to check stability given $M_{\mathcal{GP}}$ in (18) that contains the GP buffer. If the resulting closed-loop is unstable, e.g., due to modeling errors, the following slightly more conservative frequency-domain condition is provided to tune R for stability.

Corollary 1. *Theorem 2 is satisfied if*

$$M_{\mathcal{GP}}(e^{j\omega})\left(1 - S_P(e^{j\omega})L(e^{j\omega})\right) < 1, \tag{22}$$

for all $\omega \in [0, \pi]$.

Corollary 1 yields that the closed-loop is stable if (i) a perfect model is available, i.e., $LS_P^{-1} = 1$, or (ii) if model errors appear $L \neq S_P^{-1}$ then $M_{\mathcal{GP}}$ in (18) must be designed to act as a robustness filter and stabilize the closed-loop S_R, which is further addressed in Section 5.

4. Design methodology for Gaussian process RC

In this section, design guidelines are presented for the learning filter and selection of suitable prior knowledge through the covariance function κ for the class of disturbances in Definition 2. Finally, a procedure to implement GPRC is provided.

4.1. Learning filter design

The learning filter L in the repetitive controller (17) is present for stability, i.e., from Theorem 2 it follows that by designing L as

$$L = S_P^{-1}, \tag{23}$$

then $(1 - S_P L)$ renders zero satisfying Theorem 2 regardless of $M_{\mathcal{GP}}$.

Direct inversion of S_P may lead to an unstable or non-causal inverse, e.g., if P contains non-minimum phase zeros. By employing finite preview a bounded approximate inverse of S_P can be obtained, e.g., using Zero-Phase-Error-Tracking-Control (ZPETC) (Tomizuka, 1987; van Zundert & Oomen, 2017) yielding L of the form

$$L = L_c z^{n_l} \approx S_P^{-1} \tag{24}$$

where L_c is causal and z^{n_l} with $n_l \leq N$ is a possible finite preview.

A practical implementation for the non-causal L filter (24) is presented in Fig. 5, where the error is filtered with the causal part L_c yielding

$$y_d(k) = -L_c S_P(d(k) + \hat{d}_\mu(k)) + q^{-n_l}\hat{d}_\mu(k), \tag{25}$$

$$= -d(k - n_l), \tag{26}$$

where q is the forward time-shift operator, to be a delayed version of the disturbance with n_l samples. This delay is compensated by a preview in the memory $M_{\mathcal{GP}}$, i.e., the test point becomes $X_* = t(k + n_l)$, to implement the non-causal part of L.
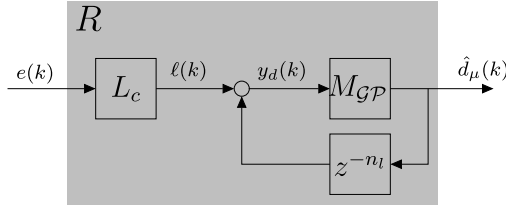
Fig. 5. Practical RC implementation with a non-causal learning filter L with causal equivalent L_c and preview z^{n_l}.

Remark 3. Note that $X_* = t(k+n_l)$ is an estimate of $\hat{d}^c$ at $t(k+n_l)$ being n_l samples in the future. This is possible by introducing smoothness in the GP prior as shown later.

4.2. Prior selection

In this section, a suitable covariance function κ in (12) that specifies prior knowledge for the class of disturbances in Definition 2 is presented.

The additive structure in Definition 2 is imposed on the disturbance model (12) by parameterizing it as a sum of n_d periodic functions with periods T_i, i.e.,

$$\hat{d}^c(t) = \sum_{i=1}^{n_d} \hat{d}_i^c(t), \text{ with } \hat{d}_i^c(t) \sim \mathcal{GP}(0, \kappa_i(t, t')), \quad (27)$$

where $\hat{d}_i^c$ are samples from n_d independent GPs with periodic covariance function κ_i. Hence, $\hat{d}^c(t)$ in (27) is referred to as an additive GP, see, e.g., Durrande, Ginsbourger, and Roustant (2011), with an additive covariance function

$$\kappa(t, t') = \sum_{i=1}^{n_d} \kappa_i(t, t'), \quad (28)$$

that is simply the sum of the individual covariance functions κ_i. The periodic covariance function κ_i is of the form

$$\kappa_i(t, t') = \sigma_{f,i}^2 \exp\left(\frac{-2\sin^2(\frac{\pi(t-t')}{T_i})}{l_i^2}\right), \quad (29)$$

with hyperparameters $\Theta_i = \{T_i, l_i, \sigma_{f,i}\}$ where

- $T_i \in \mathbb{R}$ is the period of the ith component;
- $l_i \in \mathbb{R}$ is the smoothness of $\hat{d}_i^c$, i.e., choosing l large implies less higher harmonics and vise versa; and
- $\sigma_{f,i} \in \mathbb{R}$ is a gain relative to the other components and the noise variance σ_n^2.

The periodic covariance function (29) is often encountered in literature, see, e.g., Duvenaud (2014, Chapter 2.2) and Williams and Rasmussen (2006, Chapter 4.2). Note that κ is non-periodic if there is no least common multiple as in (6) for non-periodic disturbances. An example of the periodic kernel function κ_i, and a non-periodic kernel that is a sum of two periodic kernels, including random samples taken from the prior distributions $\mathcal{N}(0, \kappa_i(t, t'))$ are shown in Fig. 6. This allows to capture both period and non-periodic disturbances in the GP-based internal disturbance model.

In GPRC with kernel function (28) the disturbance period is included through the hyperparameter T_i that may be rational, in contrast to traditional RC, allowing to reject disturbances with a rational period time. The number of components n_d specifies if the disturbance is single-period ($n_d = 1$) or multi-period ($n_d \geq 2$) and can be determined with for example a power spectral density (PSD) estimate of a measured error signal, where n_d equals the
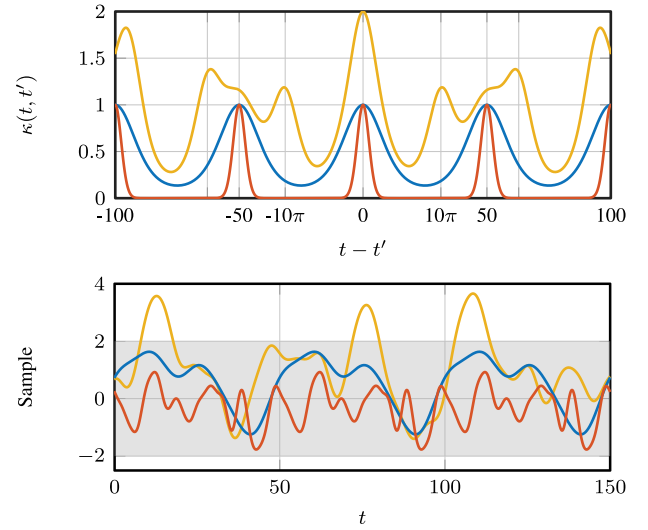

Fig. 6. Example: Top plot shows three examples of periodic covariance functions $\kappa_i(t, t')$ as a function of $t - t'$ with hyperparameters $T_1 = 50$, $l_1 = \sigma_{f,i} = 1$ in (——) and with $l_2 = 0.25$ in (——). This shows that if $t - t'$ is close to zero or the period T_i, then t and t' are highly correlated. Also the sum of two periodic kernels with periods $T_1 = 50$ and $T_2 = 10\pi$ is shown (——) yielding a non-periodic kernel function. The bottom plot shows random samples taken from the distributions $\mathcal{N}(0, \kappa_i(t, t'))$, these samples both periodic and have more (——) or less (——) smoothness, or become non-periodic (——) with a non-periodic kernel that is the sum of two periodic kernels.

number of fundamental frequencies. Finally, if the periods T_i do not have a common multiple, then the resulting kernel function is non-periodic. Hence, the prior (28) is flexible and can be tuned with only a limited number of intuitive hyperparameters.

4.3. Design procedure

The following procedure summarizes the design steps that are required to implement GP-based RC.

Procedure 1 (*GPRC design*).

Given a measured frequency response function (FRF) $\hat{S}_P(e^{j\omega})$ and a parametric model S_P, perform;

(1) Invert $\hat{S}_P$ to obtain L_c and non-causal part z^{n_l} with $n_l \geq 0$ in (24), e.g., using ZPETC.
(2) Determine n_d in (27), e.g., using a PSD estimate of the error. Then, set $i = 1$ and repeat the following.

   (a) Choose the period T_i, smoothness l_i and gain $\sigma_{f,i}$ for κ_i in (29).
   (b) until $i = n_d$, set $i \to i + 1$ and repeat step 2a.

(3) Choose a buffer size $N \in \mathbb{N}$, e.g., a good starting point is $N \geq \sum_{i=1}^{n_d} T_i$ which yields sufficient design freedom, although smaller buffer sizes are possible with appropriate prior, see Remark 4.
(4) Define

$$X = \begin{bmatrix} N & N-1 & \dots & 1 \end{bmatrix}^\top, \quad (30a)$$
$$X_* = N + n_l, \quad (30b)$$

   and evaluate κ in (28) for $\kappa(X, X)$ and $\kappa(X, X_*)$ to obtain K and K_* respectively.
(5) Compute FIR coefficient $\mu^{\mathcal{GP}}$ in (16) and verify stability with $\hat{S}_P$ using Theorem 2 or Corollary 1 (Remark 5).

Remark 4. To model a periodic signal with period T at least T independent parameters are required. By including a correlation through smoothness ($l > 0$) or periodicity in the kernel, a smaller buffer size $N < T$ can be used in practice.

Remark 5. The FIR filter $M_{\mathcal{GP}}$ influences stability if $L \neq S_p^{-1}$, it is shown in Section 5 that increasing smoothness yield more robustness for modeling errors.

5. Performance and robustness

The generic GPRC framework introduced in the previous sections is further analyzed, i.e., it is shown under which conditions traditional RC and Higher-order RC (HORC) (Steinbuch et al., 2007) are recovered as a special case of GPRC. Furthermore, by a suitable kernel choice GPRC improves robustness for period variations or reduces the sensitivity with respect to noise similar to Steinbuch et al. (2007). Furthermore, GPRC applied to multi-period disturbances and disturbances with a rational period time is analyzed.

5.1. Recovering traditional RC

GPRC recovers traditional RC for a specific type of prior, i.e., a periodic kernel without smoothness. In traditional RC the buffer $M_T = z^{-(N-n_l)}$ is a pure delay, hence, the output is simply a delayed version of the input. This is recovered in GP-based RC as follows.

Theorem 3. *In the setting in Fig. 5 and under the conditions in Theorem 1, then with $N = T \in \mathbb{N}$, a periodic kernel (28) where $n_d = 1$ and $T = N$, $\sigma_n^2 = 0$, $\sigma_f^2 = 1$, and $l \to 0$, the memory*

$$M_{\mathcal{GP}} = z^{-(N-n_l)}, \tag{31}$$

recovers traditional RC.

Proof. To show that $M_{\mathcal{GP}}(z) = z^{-(N-n_l)}$, note that this is equivalent to showing that $\hat{d}_\mu(k) = y_d(k - N + n_l)$. The output $\hat{d}_\mu(k) = \mu^{\mathcal{GP}} w(k)$ with $w(k)$ in (10), hence by showing that the vector

$$\mu^{\mathcal{GP}} = \begin{bmatrix} 0_{N-n_l-1} & 1 & 0_{n_l-1} \end{bmatrix}^\top \in \mathbb{R}^N \tag{32}$$

implies that $M = z^{-(N-n_l)}$. Substitute $\sigma_n^2 = 0$ and $\sigma_f^2 = 1$, then in the limit case the kernel function (29) is of the form

$$\lim_{l \to 0} \kappa = \lim_{l \to 0} \exp\left(\frac{a(k)}{l^2}\right) = \begin{cases} 0 \text{ if } a(k) \neq 0 \\ 1 \text{ if } a(k) = 0 \end{cases}$$

where $a(k) = -2\sin^2\left(\frac{\pi\tau(k)}{T_i}\right) = 0 \ \forall \ \tau(k) = \beta T_i$ with $\tau(k) = X(k) - X'(k)$ and $\beta \in \mathbb{Z}$. With $X(k)$ in (11) this leads to $K = I_N$ and $\lim_{\ell_i \to 0} K_*^\top K^{-1}$ is of the form (32) which completes the proof. ∎

Hence, by setting smoothness to zero and the kernel period limited to an integer, the traditional RC memory is recovered. Next, it is shown that GPRC is not limited to disturbances that have an integer period time through introducing smoothness.

Remark 6. Theorem 3 shows that setting $l \to 0$ recovers traditional RC, which does not take inter-sample behavior into account (Nagahara & Yamamoto, 2016). In the following subsections, the smoothness $l > 0$ resulting in a smooth and continuous disturbance estimate, also in-between the discrete data point, i.e., the inter-sample modeling error is reduced. In Nagahara and Yamamoto (2016), sampled-data signal reconstruction is employed to generate a continuous-time disturbance model that explicitly takes inter-sample behavior into account in RC.
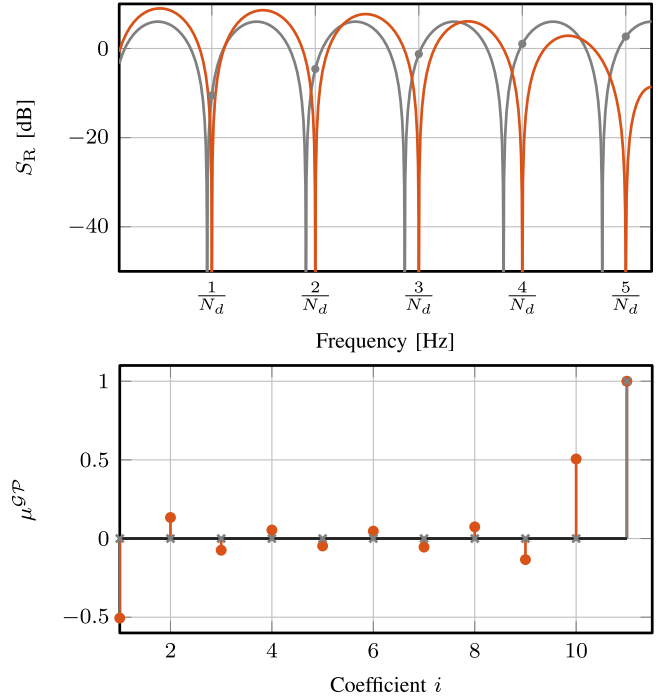

Fig. 7. Example 1: Modifying sensitivity function S_R (top plot) and impulse response of $M_{\mathcal{GP}}$ (bottom plot) for GPRC without smoothness and $T = 11$ (——), and with smoothness with $T = 10.5$ (——). Including smoothness yield that many FIR coefficients $\mu^{\mathcal{GP}}$ are non-zero (●) for automatic interpolation, which enables suppression at $1/N_d$ and higher harmonics, whereas traditional RC performance in much worse (✕).

5.2. GPRC for discrete-time non-periodic disturbances

Traditional RC is not applicable to rational period times as in Definition 2 with $T \in \mathbb{R}$ which are non-periodic in discrete time, for these disturbances additional interpolation is required, see, e.g., Cao and Ledwich (2002). In contrast, it is shown that GPRC can suppress disturbances that have a rational period time.

In GPRC the disturbance period is specified through the kernel function (29) where $T_i \in \mathbb{R}$, and is not necessarily related to the buffer size $N \in \mathbb{N}$ as in traditional RC. It is shown in Theorem 3 that if $l \to 0$ and T is an integer, then $M_{\mathcal{GP}}$ is a pure delay such that $\hat{d}_\mu$ in (19) depends solely on $y_d(k - T)$. In the case that T is rational then $y(k - T)$ is not directly available, i.e., it is in-between two samples, but it is estimated from the available inputs using a smoothness $l > 0$ also estimating the disturbance in-between samples. Hence, smoothness enables interpolation for disturbances with a rational period time as shown in the following example.

Example 1. Consider the problem of rejecting a disturbance with a rational period time $T_d = 10.5$ samples, for which the kernel (29) with $T = T_d$, $l = 10$ and $\sigma_f = 1$ is designed. The resulting modifying sensitivity S_R and the FIR coefficients $\mu^{\mathcal{GP}}$ are shown in Fig. 7. As a comparison, a traditional RC with $N = 11$ is also provided.

The modifying sensitivity S_R shows that GPRC (——) attenuates the disturbance at the fundamental frequency $1/T_d$ and its harmonics, through combining the available inputs $w(k)$ to estimate $\hat{d}^c(k - T_d)$ as in (19) with coefficients $\mu^{\mathcal{GP}}$ (●), yielding automatic interpolation. In contrast, it is evident that traditional RC (——) attenuates the disturbance at the wrong frequency $1/N$ which may even amplify the actual disturbance indicated by (●).

5.3. Recovering HORC

GPRC can improve the robustness of RC with respect to noise or uncertain period times similar to HORC, where $p \in \mathbb{N}$ buffers z^{-N} are combined, see, e.g., Pipeleers et al. (2008) and Steinbuch et al. (2007). Next, it is shown that HORC is a special case of GPRC, while at the same time the GP framework allows for substantially larger design freedom for the HORC controller. Consider the following Lemma and Theorem that provides conditions under which HORC is recovered, after which two examples illustrate the extended design freedom.

Lemma 1. *Consider GPRC under Assumption 1, then for all $(i, j) \in \{1, 2, \ldots, N\}$ and $i \neq j$ the kernel matrix $K(i, j) = 0$ if and only if its inverse $K^{-1}(i, j) = 0$.*

Proof. Under Assumption 1 the matrix $K \in \mathbb{R}^{N \times N}$ is square and symmetric $K = K^\top$. Decompose K as $U \Sigma U^\top$ where $\Sigma \in \mathbb{R}^{N \times N}$ is a diagonal matrix with singular values and $U = \begin{bmatrix} u_1^\top & u_2^\top & \ldots & u_N^\top \end{bmatrix}^\top \in \mathbb{R}^{N \times N}$ is unitary such that the row-vectors $u_i \in \mathbb{R}^{1 \times N}$ are orthogonal, i.e., $\langle u_i, u_j \rangle = \delta_{ij} \; \forall i, j$ where δ_{ij} is the Kronecker delta and $\langle \cdot, \cdot \rangle$ is the inner product defined over span$\{u_1, u_2, \ldots, u_N\}$. Furthermore, $U^{-1} = U^\top$ yielding that the inverse $K^{-1} = (U^\top \Sigma U)^{-1} = U \Sigma^{-1} U^\top$.

To show that $K(i, j) = u_i \Sigma u_j^\top = 0$ if and only if $K^{-1}(i, j) = u_i \Sigma^{-1} u_j^\top = 0$ the following property must hold

$$u_i \in \mathrm{Ker}(\Sigma u_j^\top) \Leftrightarrow u_i \in \mathrm{Ker}(\Sigma^{-1} u_j^\top) \tag{33}$$

for all $(i, j) \in \{1, 2, \ldots, N\}$ except for $i = j$, which holds true since U is unitary and by using that $\mathrm{Ker}(u_j) = \mathrm{Ker}(\Sigma u_j)$, see, e.g., Bernstein (2009, p.115), which completes the proof.

Lemma 2. *In the setting in Fig. 5 and under Assumption 1, then with the kernel (29) where $l \to 0$, $N = pT \in \mathbb{N}$ and $p \in \mathbb{N}$, the FIR filter $M_{\mathcal{GP}}$ in (18) is of the form*

$$M_{\mathcal{GP}} = \sum_{i=1}^{p} w_i z^{-(iN - n_l)}, \tag{34}$$

with weights $w_i \in \mathbb{R}$.

Proof. If $l \to 0$ and $N = pT$ then with the same reasoning as in Theorem 3 it can be shown that $K = \kappa(X, X)$ has non-zero values on the diagonal, all Nth off-diagonals and is zero elsewhere, i.e.,

$$K = \begin{cases} K(i, i + kN) \neq 0, \\ K(i + kN, i) \neq 0, \\ 0 \text{ elsewhere}, \end{cases} \tag{35}$$

with $k, i \in \mathbb{N}$ which is the same structure as $(K + \sigma_n^2)^{-1}$ using Lemma 1. Furthermore, the vector $K_*(i) \neq 0$ for $i = N - n_l + 1$ and zero elsewhere. Then, $\mu^{\mathcal{GP}}$ in (16) is of the form

$$\mu^{\mathcal{GP}} = \begin{bmatrix} 0_{N-n_l+1} & w_1 & 0_{N-1} & w_2 & \ldots & 0_{N-1} & w_N \end{bmatrix}, \tag{36}$$

which implies that $M_{\mathcal{GP}}$ is a equal to (34) which completes the proof.

Lemma 2 shows that GPRC recovers the same structure as HORC, with weights w_i for $i = 1, 2, \ldots, p$ that depend on the kernel and hyperparameters. Sections 5.3.1 and 5.3.2 illustrate that noise-robust RC and period-time robust RC in Steinbuch et al. (2007) are closely recovered with a suitable kernel function.

5.3.1. GPs for period-time robust RC

A form of HORC improves robustness for uncertain period times, which is recovered by GPRC through a locally periodic kernel, that allows for slight variations in the disturbance estimate and is given by

$$\kappa_{\mathrm{LP}}(t, t') = \exp\left(-\frac{(t - t')^2}{2l_s^2}\right) \kappa(t, t'), \tag{37}$$

where κ in (29) is the periodic kernel and l_s the local smoothness. The following example shows that noise robust HORC is closely recovered by HORC with a locally periodic kernel.

Example 2. A GPRC is designed with a buffer size $N = 3T$ where $T = 20$ and a locally periodic kernel (37) with hyperparameters $T = 20$, $\sigma_f = 1$, $l \to 0$, $l_s = 225$ and $\sigma_n^2 = 10^{-6}$ yielding weights

$$(w_1, w_2, w_2) = (2.93, -2.92, 0.98) \tag{38}$$

in Lemma 2 that closely resemble the weights obtained in Steinbuch et al. (2007). The modifying sensitivity S_R is shown in Fig. 8 for GPRC (——) and HORC (- -) which are almost identical and significantly improve disturbance rejection for a wide range compared to traditional RC (- -).

Hence, GPRC closely recovers period-time robust RC in Steinbuch et al. (2007) using a suitable kernel function with a specific smoothness.

5.3.2. GPs for noise robust RC

GPRC can improve noise robustness with respect to traditional RC by using smoothness $l > 0$ in a periodic kernel, even outperforming noise-robust HORC with a smaller buffer size. Noise robust RC as in Steinbuch et al. (2007) is recovered using a periodic kernel without smoothness $l \to 0$. This is illustrated in the following example.

Example 3. A GPRC is designed using the periodic kernel (29) without smoothness $l \to 0$ and $T = 20$, $\sigma_f = 1$ and $\sigma_n = 10^{-7}$. The buffer Γ contains $N = 3T$ samples. This results in the weights

$$(w_1, w_2, w_2) = (0.48, 0.33, 0.19), \tag{39}$$

as in Lemma 2, that closely resemble the weights for noise-robust HORC in Steinbuch et al. (2007). With the same periodic kernel where now smoothness is included $l = 100$ and the buffer size is much smaller $N = T$ samples, then noise robust HORC is outperformed.

The resulting modifying sensitivities are shown in Fig. 8 where noise-robust GPRC without smoothness (——) recovers noise-robust HORC (- -). By employing the extended design freedom in GPRC, i.e., using smoothness, then, even with a smaller buffer size (——), it outperforms HORC due to averaging over potentially up to all N samples.

Examples 3 and 2 show that HORC is recovered without smoothness and an appropriate kernel, furthermore, introducing smoothness yields additional design freedom to improve noise robustness with a much smaller buffer size than HORC. However, including smoothness also leads to less disturbance attenuation at high frequencies as shown in Fig. 9.

5.4. GPs for multi-period RC

The periodic kernel (28) in Section 4.2 also enables rejection of multi-period disturbances. Using a multi-period kernel GPRC suppresses the disturbance at specific frequencies instead of all harmonics of the common multiple, resulting in less amplification of non-periodic errors similar to Blanken et al. (2020) or Griñó and Costa-Castelló (2005) where only odd frequencies are rejected. This is illustrated in the following example.
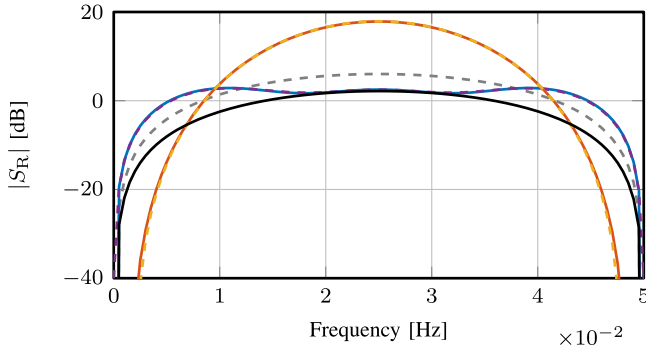
Fig. 8. Modifying sensitivity S_R with traditional RC (– –) as baseline. HORC in Steinbuch et al. (2007) for noise robustness (– –) with $N = 3T$ is recovered by GPRC a periodic kernel (—). Also HORC for period variations (– –) is recovered with a locally periodic kernel (—). Introducing smoothness (—) outperforms noise-robust HORC with a smaller buffer size $N = T$.
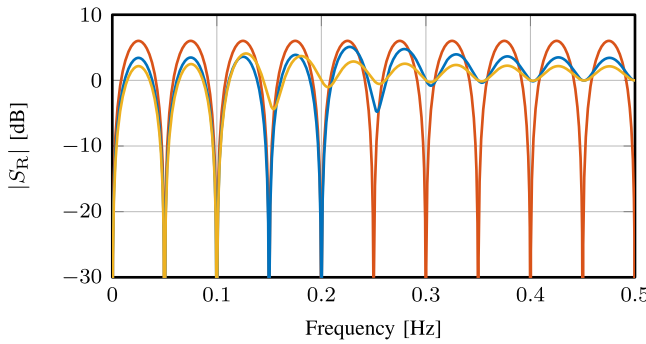

Fig. 9. Modifying sensitivity with GPRC for a periodic kernel with three different levels of smoothness $l = 10^{-6}$ (—), $l = 10$ (—) and $l = 100$ (—), showing that smoothness improves robustness for noise and reduces disturbance rejection at higher frequencies.

Example 4. The modifying sensitivity with a multi-period kernel where $n_d = 2$, $T_1 = 20$, $T_2 = 15$, and $l \to 0$ is shown in Fig. 10 for buffer size $N = T_1 + T_2 = 35$ samples (—) and for a larger buffer size $N = \text{lcm}(T_1, T_2) = 60$ samples (—).

Fig. 10 shows that only disturbances with fundamental frequencies $1/T_1$ and $1/T_2$ are suppressed, compared to traditional RC with $N = 60$ samples (—) that yield unnecessary disturbance suppression at $1/T$ and harmonics. The FIR coefficients $\mu^{\mathcal{GP}}$ in (18) are given in Fig. 11, which are non-zero at the multiples of T_1 and T_2 and the difference between both.

Example 4 illustrates that by only introducing disturbance suppression where this is required, less amplification of noise at intermediate frequencies is obtained, due to Bode's Sensitivity integral.

Remark 7. Example 4 shows that a buffer size of $N = T_1 + T_2$, as in Remark 4 is sufficient to suppress the disturbance, with more data the robustness with respect to noise is improved by averaging out over multiple samples.

Remark 8. If uncertain period times, noise and multi-period disturbances appear at the same time, then a sum of locally periodic kernels K_{LP} in (37) can be used. In this case, l_s acts tuning parameter for the trade-off between noise robustness or period-time uncertainty. Specifically, if l_s is large, then κ_{LP} has more emphasis on noise robustness, i.e., $\lim_{l_s \to \infty} \kappa_{LP} = \kappa$, and if l_s is small then period uncertainties are more taken into account.
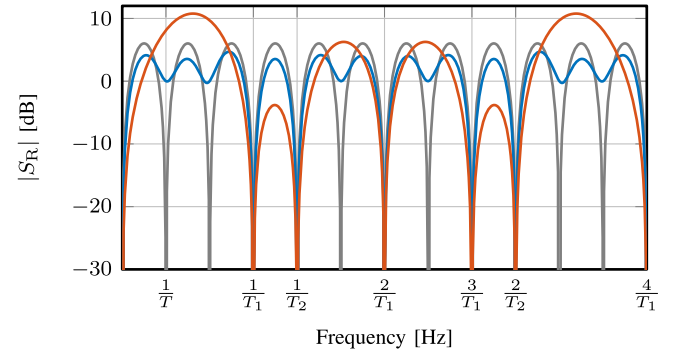

Fig. 10. Modifying sensitivity S_R for multi-period GPRC with $n_d = 2$, $T_1 = 20$ and $T_2 = 15$ samples with buffer size $N_1 = T_1 + T_2 = 35$ samples (—) and $N_2 = \text{lcm}(T_1, T_2) = 60$ samples. As a comparison, the traditional RC with $N = 60$ is also shown (—).
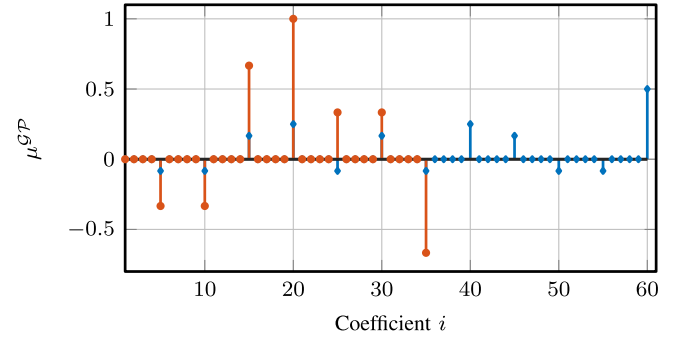

Fig. 11. FIR coefficients $\mu^{\mathcal{GP}}$ with a multi-period kernel where $n_d = 2$, $T_1 = 20$, $T_2 = 15$, yielding non-zero FIR coefficients $\mu^{\mathcal{GP}}$ at T_1, T_2 and the difference between them for $N_1 = 35$ (○) and with $N_2 = 60$ (◇).

5.5. Robustness for model errors

Robustness for model errors in RC is often improved by designing a robustness filter Q, typically a low-pass filter, that is placed in series with the buffer $M_{\mathcal{GP}}$. Next, it is shown that robustness is naturally included in GPRC by increasing smoothness. Theorem 2 provides a non-conservative stability condition where $M_{\mathcal{GP}}$ has a similar role as the traditional Q filter in RC, see, e.g., Hara et al. (1988) and Steinbuch (2002).

If smoothness $l \to 0$ and $n_d = 1$, then by Theorem 3 $M_{\mathcal{GP}} = z^{-(N-n_l)}$ which has magnitude $|M_{\mathcal{GP}}(e^{j\omega})| = 1 \forall \omega$, see (—) in Fig. 12. To improve robustness, the buffer $M_{\mathcal{GP}}(e^{j\omega}) < 1$ for the frequencies where model errors are present. In Fig. 12 $M_{\mathcal{GP}}$ is given for $l = 1$ (—) and $l = 0.5$ (—) resulting in a low-pass characteristic which increases robustness for high-frequency modeling errors.

From an intuitive point of view, higher smoothness yields a smoother disturbances estimate $\hat{d}^c$, and thereby less high-frequency content in the RC output $\hat{d}_\mu$. Hence, learning is limited in the high-frequency range, i.e., where the model is not reliable, having a similar effect as a Q filter in traditional approaches. Hence, smoothness also imposes an upper bound on the frequency content of the disturbance that can be learned.

Remark 9. The markers (●) and (●) in Fig. 12 indicate the magnitude of $M_{\mathcal{GP}}(e^{j\omega})$ for $\omega = \frac{2\pi}{T}$ and its harmonics. In between these frequencies the magnitude of $\mu^{\mathcal{GP}}\Gamma$ is small, hence disturbances at those frequencies are filtered out. Note that $M_{\mathcal{GP}} > 1$ for some frequencies, which is allowed as long as Theorem 2 is satisfied.
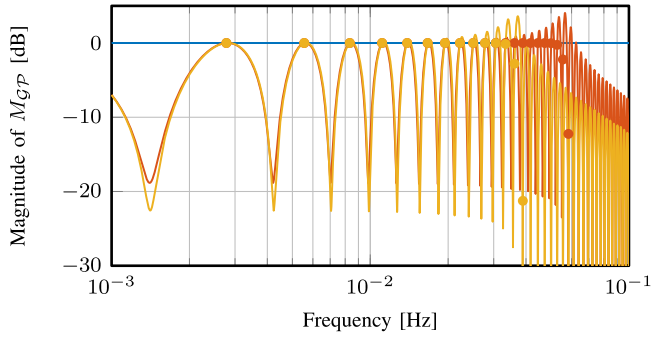
Fig. 12. Magnitude of $M_{\mathcal{GP}}$ for a periodic kernel with $n_d = 1$ and $T = 360$ and three settings of smoothness, i.e., $l = 10^{-3}$ (——), $l = 0.5$ (——) and $l = 1$ (——). The markers (●) and (●) indicate fundamental frequencies $f = \frac{1}{T}$ and harmonics (top plot). This shows that smoothness leads to a low-pass characteristic in $M_{\mathcal{GP}}$, which in turn increases robustness.

Remark 10. GPRC can be extended with a robustness filter Q if desired, i.e., $M_{\mathcal{GP}}(z) \rightarrow Q(z)M_{\mathcal{GP}}(z)$ to satisfy the stability condition (22).

6. Implementation aspects: dealing with initial conditions

The previous sections establish an LTI framework for RC synthesis using GPs. In this section, performance in the first N samples is improved even further by taking into account the initial conditions of the buffer Γ, which may limit performance in the LTI case. Two solutions are provided to avoid this.

6.1. Limitations of the LTI case

The problem that arises in the LTI case is that the initial condition of the buffer Γ, which is zero by default, appears as observations of the disturbance in the training data set $\mathcal{D}_N$ during the first N samples. Performing GP regression with these incorrect observations gives a worse disturbance estimate. After the first N samples, the initial condition of Γ disappears from the buffer. To improve GPRC in the first N samples, the following two solutions are provided.

6.2. Discarding observations

A simple solution is to discard the first N observations from the data set $\mathcal{D}_N$ that correspond with the initial conditions of the memory Γ. This is done by introducing a time-varying selection matrix Ξ_k such that $w(k) = \Xi_k \Gamma \in \mathbb{R}^{\bar{N}(t)}$ where

$$\Xi_k = \begin{bmatrix} I_{\bar{N}(t)} & 0_{\bar{N}(t) \times (N - \bar{N}(t))} \end{bmatrix} \in \mathbb{R}^{\bar{N}(t) \times N} \tag{40}$$

with $\bar{N}(t) \leq N$ the time-varying number of samples that are used for GP regression. After N samples $\bar{N}(t) = N$ thus $\Xi_k = I_N$ such that the LTI case in Theorem 1 is recovered.

Note that this approach requires computing (16) at each sample during the first N samples, which is computationally demanding. Therefore, an alternative solution is introduced next.

6.3. Time-varying kernel to improve learning

A second solution is to choose a sufficiently high noise variance $\sigma_r^2 \gg \sigma_n^2$ for the undesired inputs such that these are reflected less in the RC output. This can be done by modifying the matrix $(K + \sigma_n^2 I_N)$ in (16), by replacing the diagonal matrix with

noise variances $\sigma_n^2 I_N$ with the following time-varying diagonal matrix

$$K_v^k = S_k \sigma_r^2 + (I_N - S_k)\sigma_n^2 \tag{41}$$

where

$$S_k = \begin{bmatrix} 0_\Delta & 0 \\ 0 & I_{\bar{N}-\Delta} \end{bmatrix} \tag{42}$$

is a selection matrix in which

$$\Delta = \begin{cases} 0 & \text{if } k \leq n_l, \\ N & \text{if } k - n_l \geq N, \\ k - n_l & \text{otherwise,} \end{cases} \tag{43}$$

such that after N samples $S_k = 0_N$ and the LTI case is recovered.

The time-varying matrix K_v^k is diagonal with noise variance σ_r^2 for GP inputs that correspond to the initial condition of Γ, and the variance is σ_n^2 for the GP inputs that represent the disturbance. In this way, the observations with a large variance have negligible influence on the posterior mean (15a), resulting in a significant improvement in convergence during the first N samples if smoothness is included as shown in Section 7.

Remark 11. Both solutions lead to a time-varying system in the first N samples and are equivalent to the LTI repetitive controller in Theorem 1 after N samples.

7. Generic case study

In this section, a simulation case study is performed in the most general case, i.e., a multi-period disturbance with a rational period-time, in presence of noise, and a very large common multiple such that traditional RC methods are not directly applicable. In addition, the effect of increasing smoothness and model uncertainties is illustrated.

7.1. System and disturbance

The case study is performed in the setting in Fig. 1, where P is a discrete-time second order mass–spring–damper system given by

$$P(z) = \frac{0.05(z + 1)}{z^2 - 1.99z + 0.99}, \tag{44}$$

see Fig. 16, for which a stabilizing PD controller is designed

$$C(z) = \frac{5.0047(z + 1)(z - 0.8104)}{(z - 0.5171)(z + 0.02961)}, \tag{45}$$

resulting in a 0.1 Hz bandwidth.

A multi-period disturbance $d^c(t)$ is present that contains two fundamental periods $T_1 = 20$ samples and $T_2 = 31.5$ samples such that the common multiple is very large $T = 1260$ samples, also i.i.d. Gaussian distributed noise with $\sigma_n = 10^{-3}$ is added to the disturbance. A PSD of the disturbance is depicted in Fig. 13.

Remark 12. GPRC is also applicable if there is no common multiple, i.e., to non-periodic disturbances. In this case study, a large common multiple is chosen to compare GPRC steady-state performance with traditional RC as a benchmark.

7.2. GPRC design

The learning filter L is designed as (23) using ZPETC resulting in a causal filter L_c and a non-causal part with $n_l = 1$ sample preview.

The corresponding hyperparameters with the multi-period kernel (28) are $n_d = 2$, $T_1 = 20$, $T_2 = 31.5$, including two different
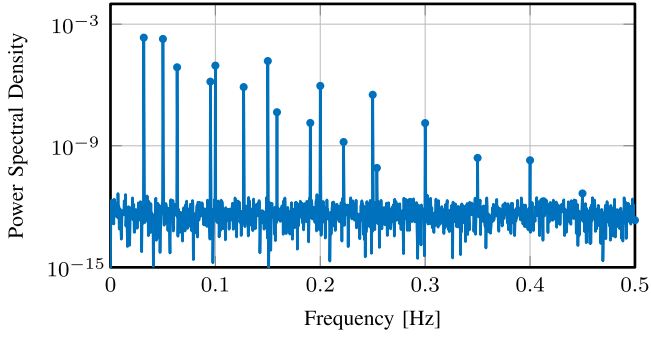
Fig. 13. Power spectral density of the multi-period disturbance, containing two fundamental periods $T_1 = 20$ samples and $T_2 = 31.5$ samples.
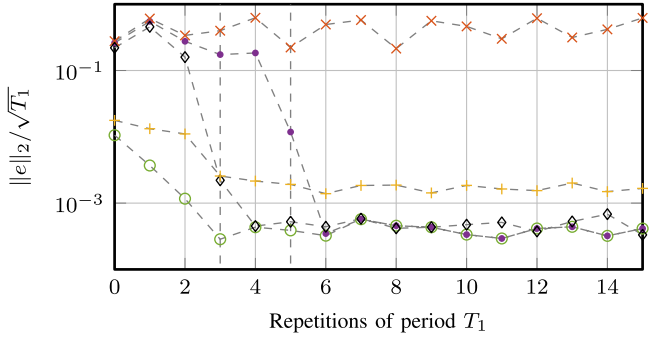

Fig. 14. Error 2-norm as function of T_1 with PD (✕). GPRC with $N_1 = 52$ in (◆) that converges after $3T_1$, and with buffer size $N_1 = 104$ (●) GPRC converges after $5T_1$. With a time-varying prior noise variance (41) the error (○) convergence is much faster ($l = 1$), converges to a larger error with a larger smoothness ($l = 3$) (+).
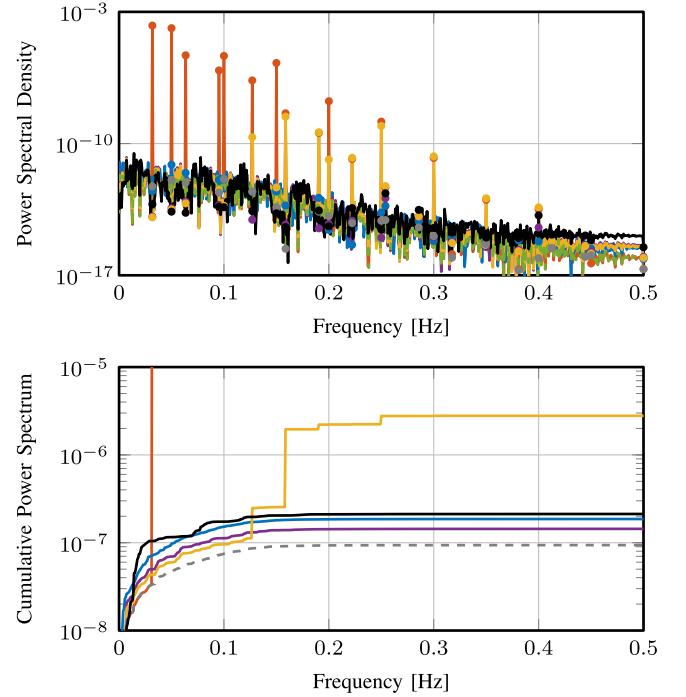

Fig. 15. Power spectral density and cumulative power spectrum of the converged error with PD (——), GPRC with buffer size $N_1 = 52$ and $l_{1,2} = 1$ as a baseline (——) that fully rejects the disturbance. In addition, with buffer size $N_2 = 104$ (——) noise is amplified less, and with too much smoothness $l_{1,2} = 3$ (——) the higher frequency harmonics are not rejection sufficiently. As a comparison traditional RC with a very large buffer size $N = \text{lcm}(T_1, T_2) = 1260$ samples (——) is outperformed by GPRC and the lower bound is given by the noise induced error (– –).

levels of smoothness $l_{1,2} = 1$ and $l_{1,2} = 3$, and $\sigma_f = 1$ and $\sigma_n = 10^{-3}$ are kept constant. The buffer Γ is implemented with two buffer sizes $N_1 = T_1 + T_2 = 52$ samples and $N_2 = 2N_1 = 104$ samples to illustrate the effect of including more data.

Simulations are conducted with PD control only, PD with LTI GPRC in Theorem 1 with the varying prior variance (41) in the first N samples where $\sigma_r = 10^3$. As a comparison, traditional RC with a buffer size $N = 1260$ is also implemented.

7.3. Results

The 2-norm of the error computed over the fundamental period T_1 is shown in Fig. 14, steady-state performance is analyzed using the power spectral density (PSD) and cumulative power spectrum (CPS) of the converged error, see Fig. 15. The following observations can be made.

- The contribution of the disturbance, i.e., the peaks in the PSD in Fig. 15 of the error without RC (——), is fully rejected by GPRC (——), that has a buffer size ($N_1 = 52$) much smaller than the period time of the disturbance ($T = 1260$). The GPRC error-norm (◆) in Fig. 14 significantly drops after $3T_1 \approx 52$ samples when sufficient observations are available (Remark 4) and the initial condition of Γ vanished from the buffer.
- Increasing the buffer size to $N_2 = 104 \ll T$ reduces the amplification of noise compared with buffer size N_1 (Section 5.3.2), yielding a lower cumulative error (——) than with N_1 (——), see Fig. 15. As a consequence of the larger buffer size the initial condition of Γ vanishes after N_2 samples yielding slower convergence as shown by the error-norm (●) in Fig. 14 that drops after $5T_1 \approx 104$ samples.

- Convergence in the first N_2 samples is significantly improved by dealing with the initial conditions using a time-varying kernel (41) (○) compared with the LTI case (●), see Fig. 14. After N_2 samples both methods have the same error.
- Increasing smoothness from $l_{1,2} = 1$ to $l_{1,2} = 3$ essentially cuts-off learning in the high-frequency range. This reduces disturbance attenuation at high-frequencies as shown by (——) in Fig. 15, and by (+) in Fig. 14.
- A perturbed model with a significant mismatch in the high-frequency range is also used to compute the learning filter, see Fig. 16. Increasing the smoothness allows to deal with this model mismatch, as discussed in Section 5.5, i.e., satisfy the stability condition in Theorem 2 as shown in the Nyquist plot in Fig. 16. The effect of increasing smoothness is discussed in the previous topic. This effect is similar to using a low-pass robustness filter in traditional RC.
- Finally, GPRC (——) can outperform traditional RC (——) both in convergence as in steady-state error while using a significantly smaller buffer.

These observations confirm that GPRC is applicable to the general case, i.e., a multi-period disturbance with a rational period time and a very large common multiple, while using only a small buffer size and a limited number of intuitive design variables. Moreover, also in practical situations, e.g., if model mismatches and noise are present, then GPRC is applicable with an appropriate kernel choice. For this example T_1 and T_2 are selected such that a comparison with traditional RC can be made, i.e., a large common multiple exists. However, in general, the existence of a common multiple is not a restriction and GPRC is readily applicable to non-periodic disturbances as well. A major advantage of GPRC is a new
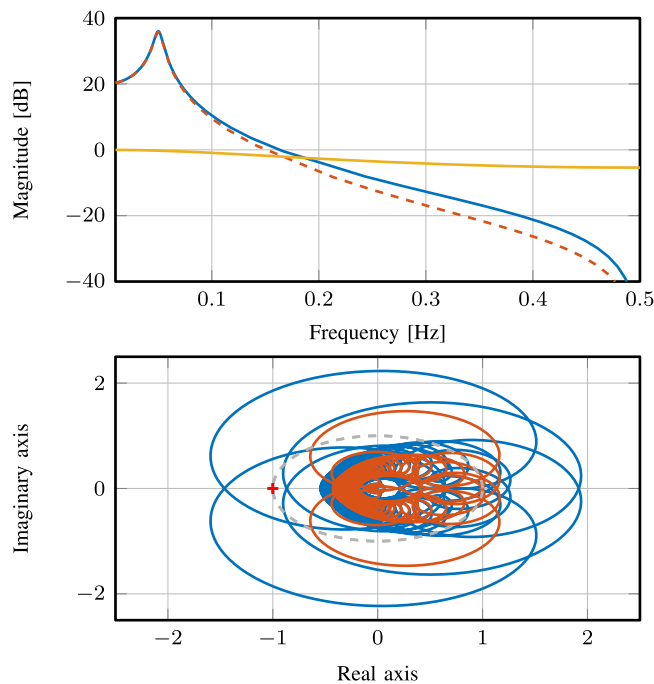
Fig. 16. Top plot shows the true system P(——), a perturbed model (- - -) that is used for RC as well as the model mismatch (——) that is significant (>100%) beyond 0.1 Hz. The bottom plot shows the Nyquist stability test for smoothness $l_1 = l_2 = 10$ (——) that is unstable, by increasing the smoothness to $l_1 = 50$ and $l_2 = 10$ the RC is stabilized (——) since there are no encirclements of the point $-1 + 0i$.

way of designing the repetitive controller that, as shown here, naturally extends to for example multi-period disturbances.

8. Conclusions

A generic repetitive control framework for asymptotic rejection of single-period, and multi-period disturbances, with potentially rational period times, is enabled through a Gaussian process (GP) based internal model. The presented GP-based approach also enables compensation within the first period, in contrast to many existing RC approaches. The disturbance is modeled using GP regression, which is a non-parametric approach that combines data with prior knowledge. Prior knowledge is included in the form of a kernel function with periodicity and smoothness, which allows modeling a wide range of disturbances by specifying intuitive tuning parameters. It appears that under mild assumptions the GP-based RC approach is LTI and more specifically given by an FIR filter, such that it is computationally inexpensive, stability conditions can be provided and several existing approaches are recovered as a special case. Moreover, applying GP-based RC for non-linear systems is conceptually possible following the developments in this paper by reformulating the stability conditions for the non-linear case which is a part of future research. Ongoing work focuses on utilizing the posterior variance of the disturbance model to improve robustness against model errors and incorrect prior.

References

Berkenkamp, F., Moriconi, R., Schoellig, A. P., & Krause, A. (2016). Safe learning of regions of attraction for uncertain, nonlinear systems with Gaussian processes. In *2016 IEEE 55th conference on decision and control (CDC)* (pp. 4661–4666).

Bernstein, D. S. (2009). *Matrix mathematics: theory, facts, and formulas.* Princeton University Press.

Bijl, H., Schön, T. B., van Wingerden, J. W., & Verhaegen, M. (2017). System identification through online sparse Gaussian process regression with input noise. *IFAC Journal of Systems and Control, 2,* 1–11.

Blanken, L., Bevers, P., Koekebakker, S., & Oomen, T. (2020). Sequential multi-period repetitive control design with application to industrial wide-format printing. *IEEE/ASME Transactions on Mechatronics, 25*(2), 770–778.

Cao, Z., & Ledwich, G. F. (2002). Adaptive repetitive control to track variable periodic signals with fixed sampling rate. *IEEE/ASME Transactions on Mechatronics, 7*(3), 378–384.

Chang, W. S., Suh, I. H., & Oh, J. H. (1998). Synthesis and analysis of digital multiple repetitive control systems. In *Proceedings of the 1998 American control conference. ACC, Vol. 5* (pp. 2687–2691). IEEE.

Cuiyan, Li, Dongchun, Zhang, & Xianyi, Zhuang (2004). A survey of repetitive control. In *2004 IEEE/RSJ international conference on intelligent robots and systems (IROS)(IEEE Cat. No. 04CH37566), Vol. 2* (pp. 1160–1166). IEEE.

Durrande, N., Ginsbourger, D., & Roustant, O. (2011). Additive kernels for Gaussian process modeling. arXiv preprint.

Duvenaud, D. (2014). *Automatic model construction with gaussian processes* (Ph.D. thesis), University of Cambridge.

Francis, B. A., & Wonham, W. M. (1976). The internal model principle of control theory. *Automatica, 12*(5), 457–465.

Goodwin, G. C., & Sin, K. S. (2014). *Adaptive filtering prediction and control.* Courier Corporation.

Griñó, R., & Costa-Castelló, R. (2005). Digital repetitive plug-in controller for odd-harmonic periodic references and disturbances. *Automatica, 41*(1), 153–157.

Hara, S., Yamamoto, Y., Omata, T., & Nakano, M. (1988). Repetitive control system: A new type servo system for periodic exogenous signals. *IEEE Transactions on Automatic Control, 33*(7), 659–668.

Mazzoleni, M., Scandella, M., Formentin, S., & Previdi, F. (2020). Enhanced kernels for nonparametric identification of a class of nonlinear systems. In *2020 European control conference (ECC)* (pp. 540–545).

Merry, R. J. E., Kessels, D. J., Heemels, W. P. M. H., van de Molengraft, M. J. G., & Steinbuch, M. (2011). Delay-varying repetitive control with application to a walking piezo actuator. *Automatica, 47*(8), 1737–1743.

Mooren, Noud, Witvoet, Gert, & Oomen, Tom (2020). Gaussian process repetitive control for suppressing spatial disturbances. *IFAC-PapersOnLine, 53*(2), 1487–1492.

Murphy, K. P. (2012). *Machine learning: a probabilistic perspective.* MIT Press.

Nagahara, M., & Yamamoto, Y. (2016). Digital repetitive controller design via sampled-data delayed signal reconstruction. *Automatica, 65,* 203–209.

Pérez-Arancibia, N. O., Tsao, T. C., & Gibson, J. S. (2010). A new method for synthesizing multiple-period adaptive–repetitive controllers and its application to the control of hard disk drives. *Automatica, 46*(7), 1186–1195.

Pillonetto, G., & De Nicolao, G. (2010). A new kernel-based approach for linear system identification. *Automatica, 46*(1), 81–93.

Pipeleers, G., Demeulenaere, B., de Schutter, J., & Swevers, J. (2008). Robust high-order repetitive control: optimal performance trade-offs. *Automatica, 44*(10), 2628–2634.

Scampicchio, A., Chiuso, A., Formentin, S., & Pillonetto, G. (2019). Bayesian kernel-based linear control design. In *2019 IEEE 58th conference on decision and control (CDC)* (pp. 822–827).

Schiff, J. L. (1999). *The laplace transform: theory and applications.* Springer Science & Business Media.

Shan, Y., & Leang, K. K. (2012). Accounting for hysteresis in repetitive control design: Nanopositioning example. *Automatica, 48*(8), 1751–1758.

Shi, Y., Longman, R. W., & Nagashima, M. (2014). Small gain stability theory for matched basis function repetitive control. *Acta Astronautica, 95,* 260–271.

Skogestad, S., & Postlethwaite, I. (2007). *Multivariable feedback control: analysis and design, Vol. 2.* Citeseer.

Steinbuch, M. (2002). Repetitive control for systems with uncertain period-time. *Automatica, 38*(12), 2103–2109.

Steinbuch, M., Weiland, S., & Singh, T. (2007). Design of noise and period-time robust high-order repetitive control, with application to optical storage. *Automatica, 43*(12), 2086–2095.

Tomizuka, M. (1987). Zero phase error tracking algorithm for digital control. *Journal of Dynamic Systems, Measurement, and Control, 109*(1), 65–68.

Umlauft, J., Beckers, T., Capone, A., Lederer, A., & Hirche, S. (2020). Smart forgetting for safe online learning with Gaussian processes. In *Learning for dynamics and control* (pp. 160–169). PMLR.

Williams, C. K., & Rasmussen, C. E. (2006). *Gaussian processes for machine learning, Vol. 2.* Cambridge, MA: MIT Press.

Zhou, K., Wang, D., Zhang, B., Wang, Y., Ferreira, J. A., & de Haan, S. W. H. (2007). Dual-mode structure digital repetitive control. *Automatica, 43*(3), 546–554.

van Zundert, J., & Oomen, T. (2017). Inverting nonminimum-phase systems from the perspectives of feedforward and ILC. In *20th world congress of the international federation of automatic control* (pp. 12607–12612).

Noud Mooren received his B.Sc. degree from Fontys University of Applied Sciences, and M.Sc. degree (cum laude) from the Eindhoven University of Technology, both in Eindhoven, The Netherlands. He is currently a Ph.D. candidate at the Eindhoven University of Technology. He is a recipient of the 2020 AMC Best Paper Award. His research interest is in the field of motion control and learning control techniques for applications in mechatronic systems.

Gert Witvoet received the M.Sc. degree (cum laude) and Ph.D. degree from the Eindhoven University of Technology, Eindhoven, The Netherlands. He is a senior dynamics and control specialist at the Netherlands Organisation for Applied Scientific Research (TNO), Delft, The Netherlands, and a part-time assistant professor with the Mechanical Engineering department at the Eindhoven University of Technology. He is a recipient of the Unilever Research Prize, and several best Master teacher awards. His research interests are in the application of advanced motion control techniques on high-tech instruments and applications in the semiconductor, astronomy, and space markets.

Tom Oomen received the M.Sc. degree (cum laude) and Ph.D. degree from the Eindhoven University of Technology, Eindhoven, The Netherlands. He is currently a professor with the Department of Mechanical Engineering at the Eindhoven University of Technology. He is also a part-time full professor with the Delft University of Technology. He held visiting positions at KTH, Stockholm, Sweden, and at The University of Newcastle, Australia. He is a recipient of the 7th Grand Nagamori Award, the Corus Young Talent Graduation Award, the IFAC 2019 TC 4.2 Mechatronics Young Research Award, the 2015 IEEE Transactions on Control Systems Technology Outstanding Paper Award, the 2017 IFAC Mechatronics Best Paper Award, the 2019 IEEJ Journal of Industry Applications Best Paper Award, and recipient of a Veni and Vidi personal grant. He is Associate Editor of the IEEE Control Systems Letters (L-CSS), IFAC Mechatronics, and IEEE Transactions on Control Systems Technology. He is a member of the Eindhoven Young Academy of Engineering. His research interests are in the field of data-driven modeling, learning, and control, with applications in precision mechatronics.